USDA NATURAL RESOURCES CONSERVATION SERVICE **COLORADO**


high soil burn severity, 9/4/2012


Pendergrass Creek watershed, 9/4/2012

HIGH PARK FIRE: Increased Flood Potential Analysis

October 2012


upper Rist Canyon, 7/9/2012


Hill Gulch in Poudre Park, 7/8/2012

NRCS

Helping People Help the Land

U.S. DEPARTMENT OF AGRICULTURE
NATURAL RESOURCES CONSERVATION SERVICE
COLORADO STATE OFFICE

October 26, 2012

HIGH PARK FIRE: Increased Flood Potential Analysis

Location: Larimer County, Colorado

Summary: The High Park Fire, in the foothills west of Fort Collins, burned more than 87,000 acres between June 9th and July 1st, 2012. Increased flooding and debris flows have since occurred in streams draining numerous portions of the fire. For the next several years substantially increased flood peaks, flow volumes, sediment transport and stream channel destabilization are expected in streams draining the fire area.

The NRCS curve number (CN) technique was implemented for estimating direct runoff from rain events for both pre- and post-fire conditions. The purpose of this modeling was to develop estimates of flood hazard potential and potential threat to life and property along streams draining the fire. These results are reasonable predictions for the determination of current infrastructure sufficiency for passing increased flood flows, as well as allow the design of new infrastructure. These results can also be used to compute values useful for stream stability assessment. The High Park Fire Burned Area Emergency Response (BAER) report presented an initial hydrologic analysis of flood increases to be expected from the fire. However, this assessment was performed with a number of simplifications required to meet the aggressive timeline dictated by the BAER process. This report details additional hydrologic analyses performed to support the needs of engineers, planners, and emergency response personnel.

In many catchments, the 10-year rain event on post-fire landscapes has been predicted to cause 50- or 100-year (pre-fire condition) floods. As a result, for smaller, substantially-burned catchments, there is more than a 40 percent chance of having a (pre-fire condition) 50- or 100-year flood in the next 5 years. Due to the limited spatial extent of convective storms, the flood response will likely decrease as catchment size increases.

Watershed maps for each modeled catchment are presented in Appendix A of this report. The maps illustrate computation points, soil burn severity, and 10-year hydrographs at the stream outlets. Tables with expected pre- and post-fire peak flows, sediment bulking flows, and post/pre fire peak flow ratios for the 2-, 10-, 25-, 50- and 100-year rain events are also provided on these watershed maps. A poster illustrating increased flood potential of most streams draining the fire, through post/pre flow ratios, was also developed.

PREPARED BY: ______________________ **DATE:** 10/26/2012

STEVEN E. YOCHUM, PhD, PE
Hydrologist
970-295-5657, steven.yochum@co.usda.gov

TABLE OF CONTENTS

LIST OF FIGURES

LIST OF TABLES

INTRODUCTION

The High Park Fire (Figure 1), in the foothills west of Fort Collins, burned more than 87,000 acres between June 9th and July 1st, 2012, the day containment was declared. Increased flooding and debris flows have since been reported in streams draining numerous portions of the fire, with local residents noting that some of these floods have been the most severe since the Big Thomson flood of 1976. For the next several years substantially increased flood peaks, flow volumes, sediment transport, and stream channel destabilization are expected in streams draining the fire area.

Wildfires cause hydrologic shifts for a number of years. Substantially increased runoff and sediment production result from the loss of vegetation, soil cover, and hydrophobicity, where the fire-induced vaporization of hydrophobic compounds cause water to collect on the soil surface and runoff, instead of infiltrate. The lack of vegetation interception and soil infiltration, from the loss of surface roughness from ground litter and hydrophobicity, shifts the rainfall response from infiltration-dominated processes to surface runoff-dominated processes. For example, the runoff response from a 10-year rain event on a wildfire-impacted catchment in Switzerland shifted the flood response to a 100- or 200-year event, due to changes in infiltration capacity (Conedera et al. 2003), though scale effects with greater runoff enhancement in smaller catchments and tendencies towards overestimation in larger catchments have been noted (Stoof et al. 2011). Hydrophobicity, which tends to be more prevalent with increased sand content and lower soil water content, has been found to weaken within a few months of a fire but persist for at least 22 months in ponderosa and lodgepole pine forests of the Colorado Front Range (Huffman et al. 2001). Post-fire sediment yield is most dependent on ground cover, with percent ground cover explaining more than 80 percent of the variability in sediment yield (Benavides-Solorio and MacDonald 2001). Soil burn severity is hence fundamental for predicting sediment yield increases.

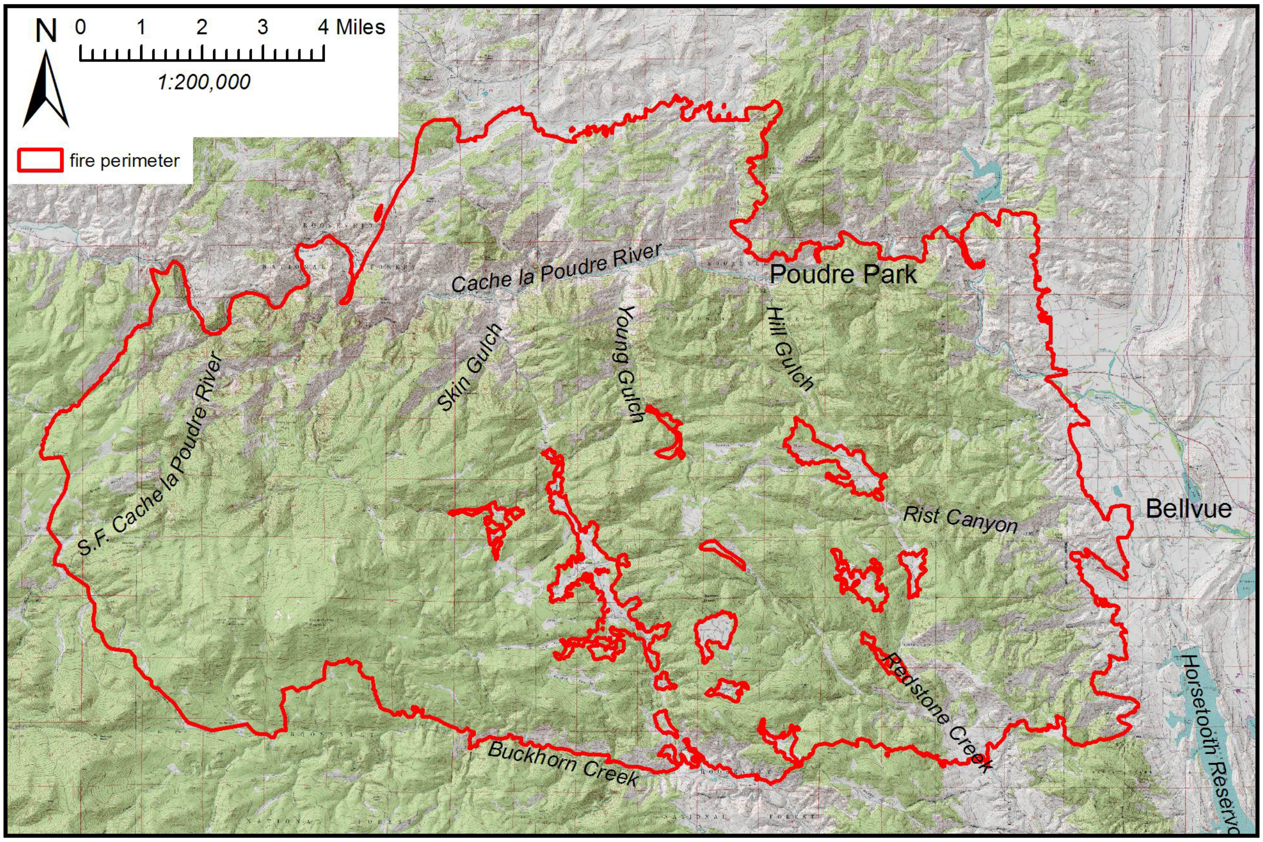

Figure 1: High Park Fire burn area extent.

The High Park Fire Burned Area Emergency Response (BAER) report (BAER 2012) presented an initial hydrologic analysis of flood increases to be expected from the fire. However, this assessment was performed with a number of simplifications required to meet the aggressive timeline dictated by the BAER process.

This complimentary NRCS report details additional hydrologic analyses performed to assess the expected magnitude of flood increases in populated areas at risk of loss of life and property. These flood predictions are more appropriate for use by engineers, planners, and emergency response personnel.

The principal results are provided in tabular form within figures illustrating individual streams draining the fire. Both post and pre peak flows are presented, to allow engineers and emergency response personnel the capability to choose from within a range of flows what the expected flood response may be during the wildfire recovery process. These maps are provided as Appendix A to this report. Additionally, a poster was developed that shows increased flood potential of most streams draining the fire. These results, presented as ratios of predicted post/pre fire peak flow burn ratios for the 25-year rain event, provide a comprehensive summary of the expected relative flood enhancement response of the fire.

METHODS

Hydrologic modeling was performed using the program HEC-HMS (version 3.5), a model developed by the U.S. Army Corps of Engineers' Hydrologic Engineering Center. The NRCS curve number (CN) technique for estimating direct runoff from rain events was used in this analysis. Catchments and modeled stream channels implemented in the analyses are presented in Figure 2. As quality control, peak flows estimated using the USGS regression equations (Capesius and Stephens 2009), embedded in USGS Streamstats, were compared to the CN runoff results for unburned conditions.

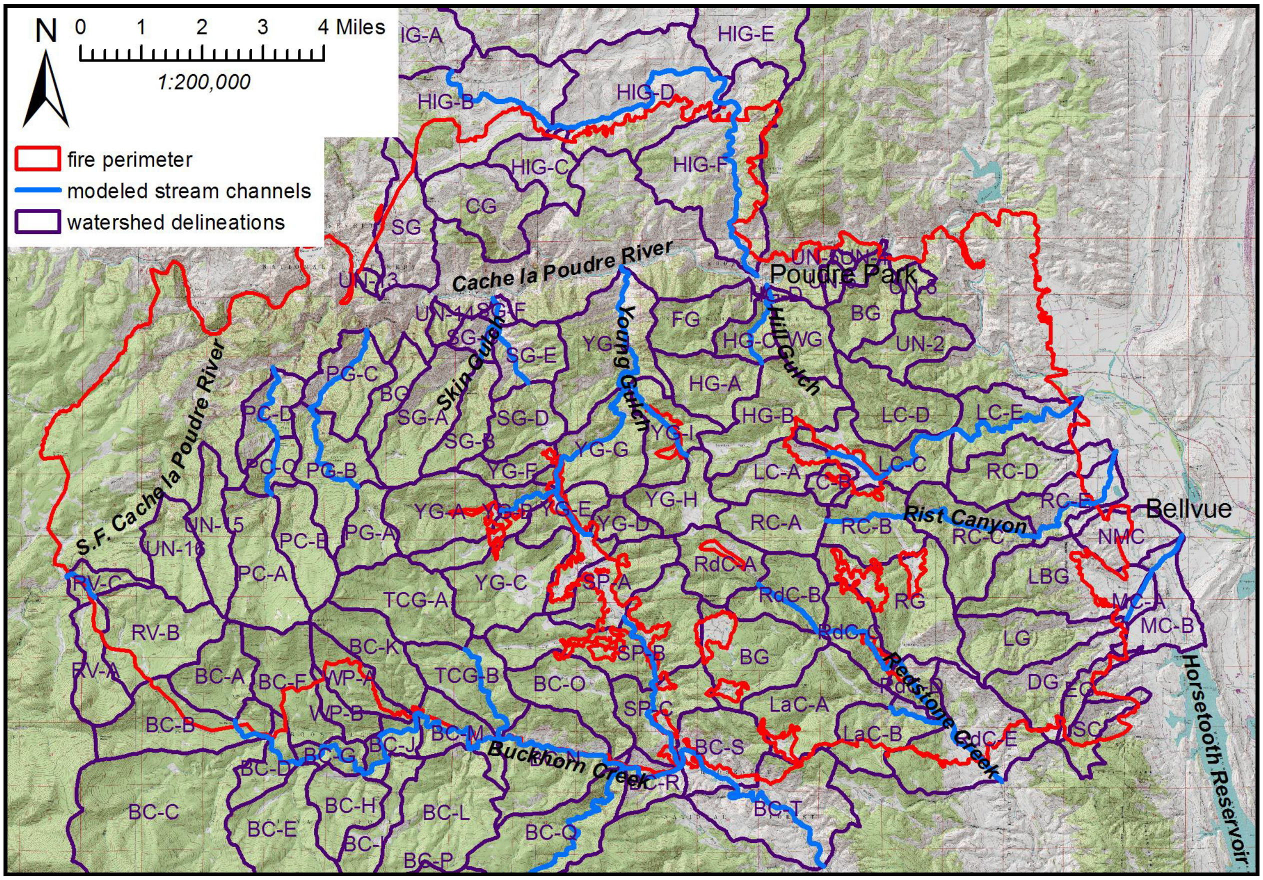

Figure 2: Modeled catchments and stream channels.

Model

As documented in NRCS (2004b), the NRCS method for estimating direct runoff from individual storm rainfall events is of the following form:

$$Q = \frac{(P - I_a)^2}{(P - I_a) + S} \qquad \text{if } P > I_a$$

$$Q = 0 \qquad \text{if } P \le I_a$$

where Q is the depth of runoff (inches), P is the depth of rainfall (inches), I_a is the initial abstraction (inches), and S is the maximum potential retention (inches). The equation derivation is not physically based but does respect conservation of mass (NRCS 2004b).

The Curve Number (*CN*) is defined as:

$$CN = \frac{1000}{10 + S}$$

The initial abstraction was initially described and has traditionally been used as:

$$I_a = 0.2S$$

The CN is a simple catchment-scale method that gives simplified results at a watershed outlet, with more accurate results expected for larger, higher-intensity rain events. The method is documented is in the NRCS National Engineering Handbook, Section 4, Hydrology, Chapters 9 and 10 (NRCS 2004a, NRCS 2004b), in Rallison (1980), as well as in numerous other publications. However, little quantitative information has been published of the database on which it was developed (Maidment 1992) and many of the curves used in the development have been misplaced (Woodward 2005). In general, the method was developed for rural watersheds in various parts of the United States, within 24 states; was developed for single storms, not continuous or partial storm simulation; and was not intended to recreate a specific response from an actual storm (Rallison, 1980).

Fundamentally, the conceptual foundation of the CN technique can be disconnected with physical streamflow generating processes during more-frequent small to moderate rain events in forested watersheds, where saturation excess overland flow can be dominant. The CN technique generally assumes that catchment runoff is driven by infiltration-excess or Hortonian overland flow. With infiltration-excess overland flow, surface runoff is generated when rainfall intensity is greater than soil infiltration capacity (as the general form of the CN model indicates), which is generally more applicable in arid and semi-arid regions and during higher rainfall intensities. Saturation excess overland flow produces runoff where rainfall depths exceed the soil capacity to retain water and becomes saturated. With saturation-excess overland flow, small to moderate rain events produce runoff from relatively small and variable portions of a catchment (variable source area hydrology). These two processes are illustrated in Figure 3.

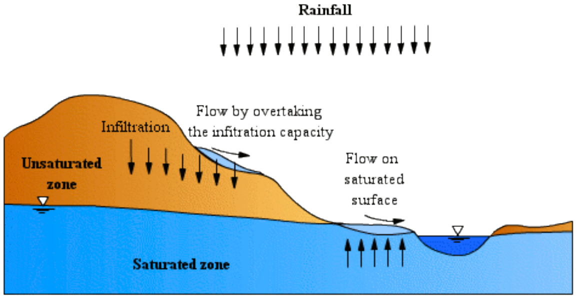

Figure 3: Hillslope section illustrating infiltration excess and saturation excess overland flow (Laboratory of Ecohydrology, EPFL).

Saturation excess overland flow can be typically dominant in forested watersheds for frequent (shallow) rain events while in burned catchments the dominant process can shift towards infiltration-excess overland flow, as indicated by such features as surface rilling on freshly-burned catchment slopes. Hence, with the application of CN hydrologic analysis to assess fire-induced enhanced runoff, the greatest uncertainty in modeling results is for frequent (shallow) rainfall events in pre-fire conditions and the best prediction are made for less frequent (deeper) rainfall events in post-fire conditions. However, post-fire conditions require use of CNs known with less certainty. Additionally, spatial rainfall variability can lead to additional modeling uncertainty. Hence, prediction error can be understood as variable depending upon rainfall depth, intensity, burn severity and catchment area, but the expected prediction error can not be specifically quantified.

Despite these shortcomings, the CN method is the preferred tool for predicting flow response of wildfire areas. This is due to its relative simplicity and achievable data requirements on large scales, and reasonable results when qualitatively compared to actual post-fire runoff events.

CN

Curve numbers are values less than 100, with higher values corresponding to catchments with lower infiltration rates and higher runoff potential. In general, CN assignments are typically made using guidance provided in NRCS (2004a).

CNs were assigned throughout the modeled catchments according to hydrologic soil group, vegetative type, soil burn severity, and ground cover condition (percent cover). Soil burn severity is a dominant factor in CN assignments in burned areas. The average catchment CN was computed using an aerial averaging methodology. Hence, catchment size was limited to areas that have similar runoff characteristics, to provide the most reliable results. As catchment size increased, CNs were computed for adjacent and serial catchments and flows were routed downstream and combined with lower catchments to predict flow at downstream points of interest. This was necessary to account for catchment shape and stream channel attenuation.

The methods used to quantify CN assignments are discussed in the following subsections.

Soil Burn Severity

Soil burn severity is the principle driver for increasing flow in runoff predictions. For this modeling, soil burn severity was measured using the BARC process from satellite data collected on 7/20/2012 (Figure 4), by researchers at Colorado

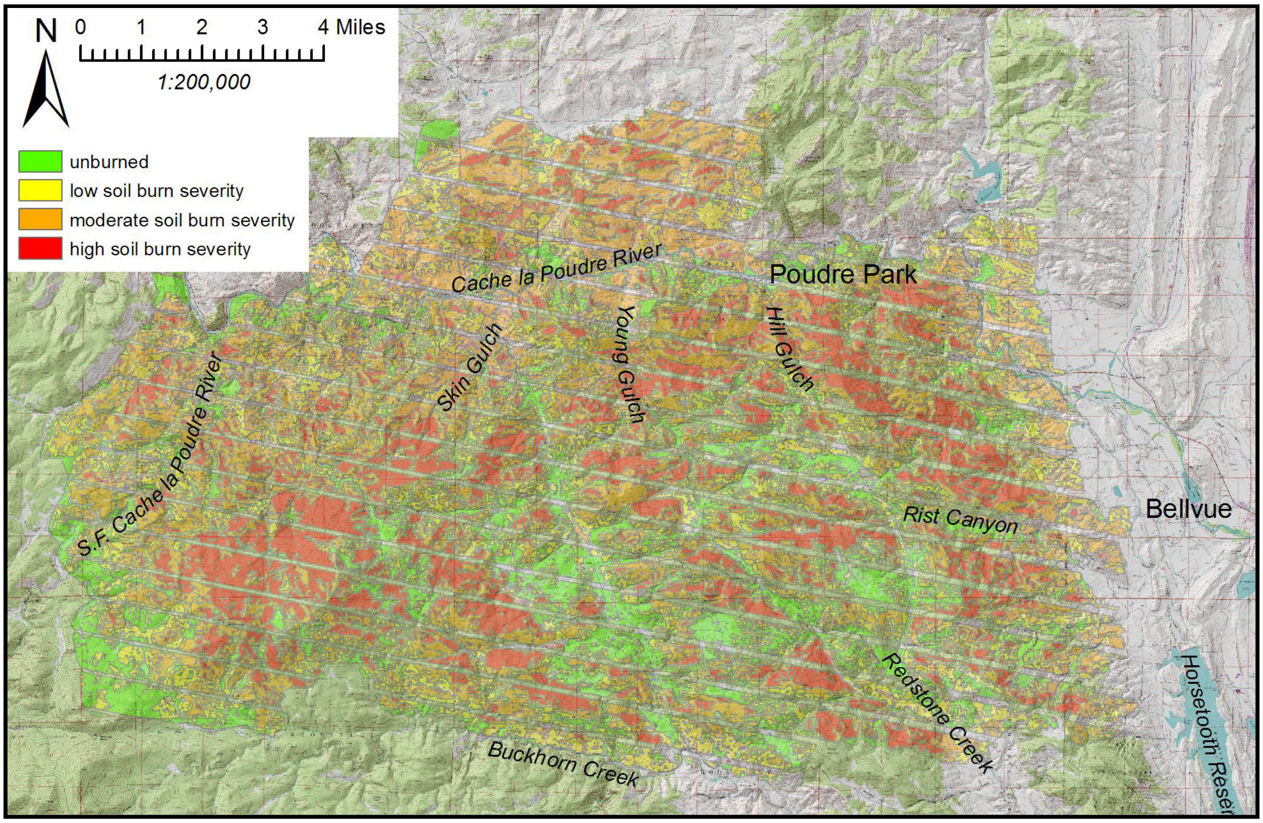

Figure 4: High Park Fire soil burn severity map, as provided by the Colorado State University.

State University. BARC (Burned Area Reflectance Classification) use reflectance recorded in satellite images to quantify soil burn severity. For defining soil burn severity, BARC images have the advantages of being comprehensive and relatively-rapidly developable. However, comparison with field-collected data has indicated that this remotely-sensed product can be more indicative of post-fire vegetative condition than soil condition, especially in low to moderately burned areas (Hudak et al. 2004). Qualitative field assessment of this High Park Fire BARC image indicates that it appears to reasonably predict burn severity in high and moderate areas.

Of note in Figure 4 is the readily-apparent banding, which is a result of a hardware glitch on Landsat 7 that fails to correct for the motion of the spacecraft as it collects images of the Earth's surface. For the purpose of this analysis, these gaps were filled through interpolation.

Hydrologic Soil Groups

Hydrologic soil group (HSG) classification was selected using soils data published in the NRCS SSURGO (Soil Survey Geographic) database. Two soil surveys cover the fire extent: NRCS Larimer County survey (CO644), published in 1980; and USFS Arapahoe-Roosevelt survey (CO 645), published in 2001. The USFS survey covers the western 1/3 of the fire (Figure 5). Using this method, soil are classified as being either A, B, C, or D type, where A allows the most infiltration and least runoff and D allows the least infiltration and greatest runoff.

As illustrated in Figure 5, greater infiltration is indicated from the USFS soil survey, with infiltration commonly increasing by a step at the survey boundary and a large area with HSG A indicated. This may be due to shallow, permeable soils over bedrock dominating the classification. This can result in substantial repercussions in the CN method, with underprediction of runoff and zero runoff prediction for more frequent (shallower) rain events.

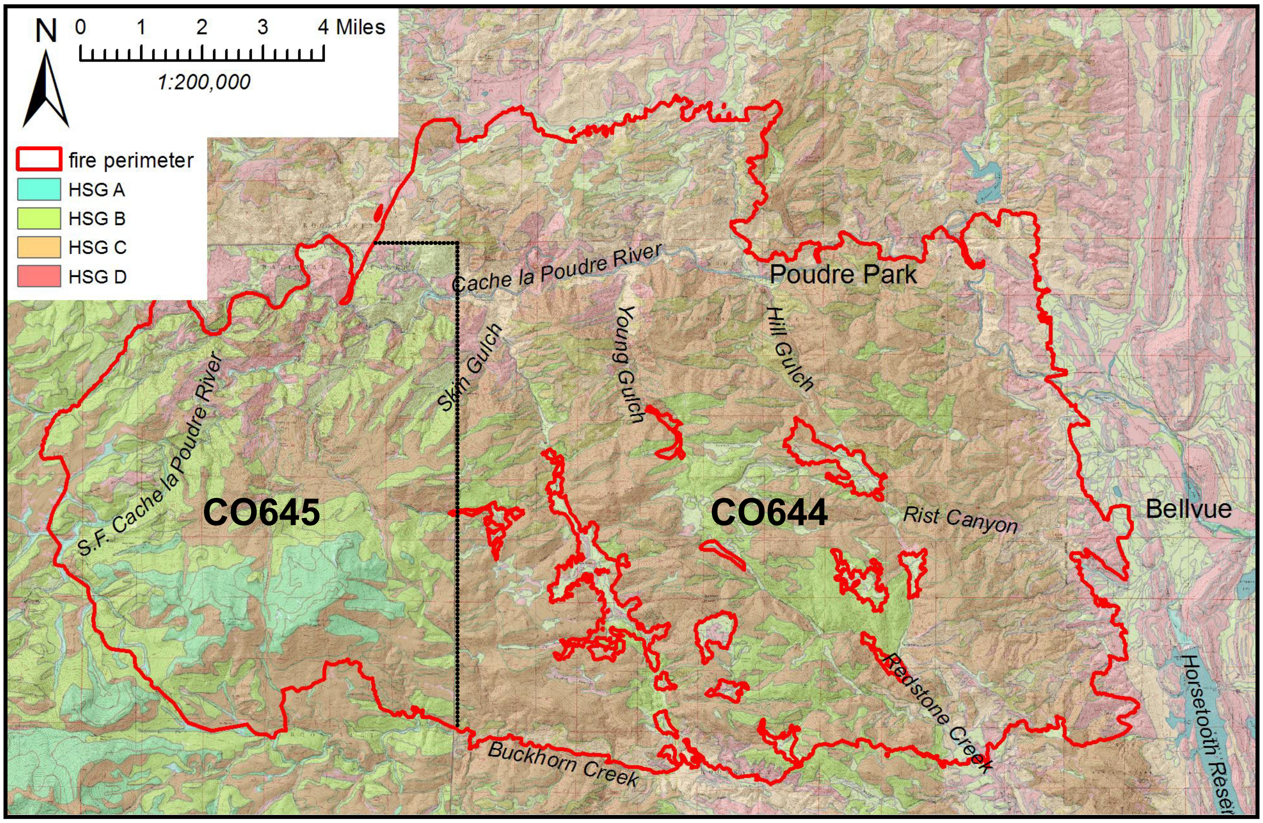

Figure 5: Hydrologic soil group (HSG) classifications utilized in the modeling.

Vegetation Type

Vegetation type, from SWReGAP (Southwest Regional Gap Analysis Project) land cover mapping, was included in the CN assignments used for the modeling. The dominant vegetation types within the fire boundary were ponderosa, lodgepole, mixed conifer, shrubs and grass (Figure 6).

CN Assignments

Curve numbers were assigned by polygons that had unique values of hydrologic soil group, vegetation type, and soil burn severity, providing more than 51,000 polygons for the entire modeled extent. In contrast to this modeling, the BAER modeling did not account for vegetation variability and clumped moderate and high soil burn severity areas. In this analysis, vegetative type was also included in the evaluation of CN and moderate and high severity areas were not clumped but instead assigned separate values.

Using primarily a compilation developed for the North Fork Fire by the NRCS, the implemented CN values are provided in Table 1. A fair ground cover condition was assumed. These values were primarily compiled from various grey literature and unpublished sources; they should be considered approximate with more research needed for post-fire CN assignments.

Rainfall

Rainfall depths used in the modeling were extracted from NOAA Atlas 2, Volume 3 (Miller et al. 1973). The rainfall distribution was identical to that used in the BAER modeling. This distribution is shown in Figure 7.

For catchments with drainages areas ≥ 6 mi^2, an aerial reduction factor was applied as detailed in Miller et al. 1973. Reduction varied from 0.95 (Skin Gulch) to 0.78 (Buckhorn Creek). When applied, this area reduction was implemented in all catchments; flow may be underpredicted in the smaller, upper catchments of such drainages.

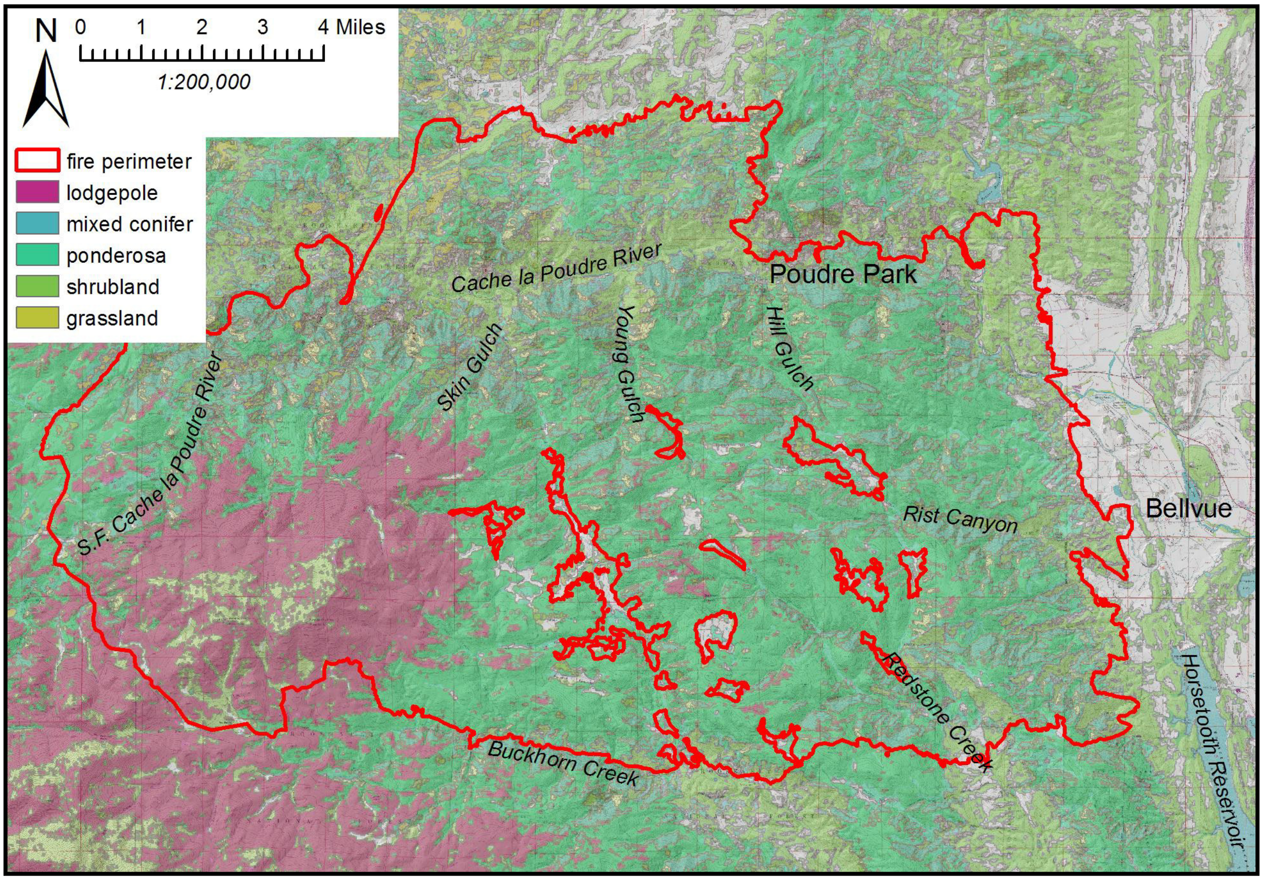

Figure 6: Dominant vegetation.

Table 1: CN assignments implemented in the High Park Fire hydrologic modeling.

Cover Description	Ground Cover Condition	A HSG				B HSG				C HSG				D HSG			
		Unburned	Low	Moderate	High	Unburned	Low	Moderate	High	Unburned	Low	Moderate	High	Unburned	Low	Moderate	High
Herbaceous—mixture of grass, weeds and low-growing brush, with brush the minor element	Poor	68	72	75	80	80	85	87	89	87	88	90	92	93	93	95	98
	Fair	49	55	67	77	71	75	80	86	81	85	88	89	89	90	90	95
	Good	39	50	65	75	62	70	75	85	74	80	81	88	85	88	89	90
Oak-aspen—mountain brush mixture of oak brush, aspen, mountain mahogany, bitter brush, maple, and other brush	Poor	48	60	72	80	66	70	75	87	74	80	85	92	79	85	90	95
	Fair	35	45	65	77	48	55	65	86	57	75	75	89	63	70	80	92
	Good	30	40	60	75	30	35	50	85	41	60	65	88	48	55	70	92
Ponderosa pine-juniper (grass understory)	Poor	45	60	72	80	75	80	84	87	85	90	91	92	89	90	92	95
	Fair	36	45	65	77	58	65	75	86	73	80	80	89	80	85	90	92
	Good	30	40	60	75	41	50	60	85	61	65	75	88	71	75	80	92
Sagebrush (grass understory)	Poor	48	60	72	80	67	70	80	87	80	85	90	92	85	90	92	95
	Fair	35	45	65	77	51	60	75	86	63	70	75	89	70	75	85	92
	Good	30	40	60	75	35	40	60	85	47	55	65	88	55	60	70	92
Lodgepole Pine Forest	Poor	45	60	72	80	66	70	75	87	77	83	85	92	83	90	92	95
	Fair	36	45	65	77	60	65	70	86	73	80	80	89	79	85	85	92
	Good	30	40	60	75	55	60	65	85	70	75	75	88	77	80	80	92
Bare soil	n/a	77	77	77	77	86	86	86	86	91	91	91	91	94	94	94	94
Wetland	n/a	98	98	98	98	98	98	98	98	98	98	98	98	98	98	98	98

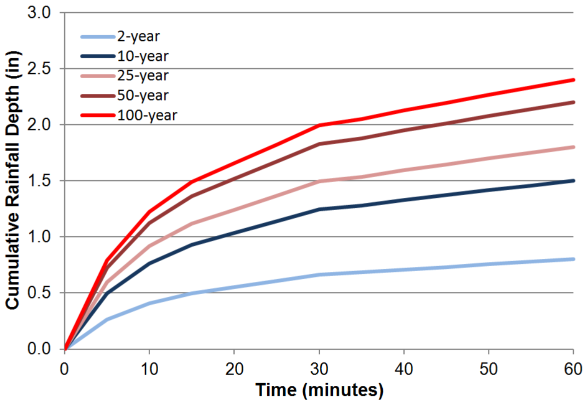

Figure 7: Cumulative rainfall distributions implemented in modeling.

Lag Time

Lag time (L), which is required to generate a hydrograph using the NRCS unit hydrograph methodology, was computed using the watershed lag method (NRCS 2010). The lag equation is:

$$L = \frac{l^{0.8}(S+1)^{0.7}}{1900Y^{0.5}}$$

, where l is the flow length (ft), Y is the average watershed land slope (%), and S is the maximum potential retention (in),

$$S = {}^{1000}\!/_{cn'} - 10$$

, where *cn'* is the retardance factor and is approximately equal to the *CN*. This method allows the computation of differing lag times for pre- and post-fire conditions, reflecting actual physical mechanisms of more rapid flow response during post-fire conditions.

Lag time, and the related time of concentration, are shown on the dimensionless unit hydrograph schematic illustrated in Figure 8.

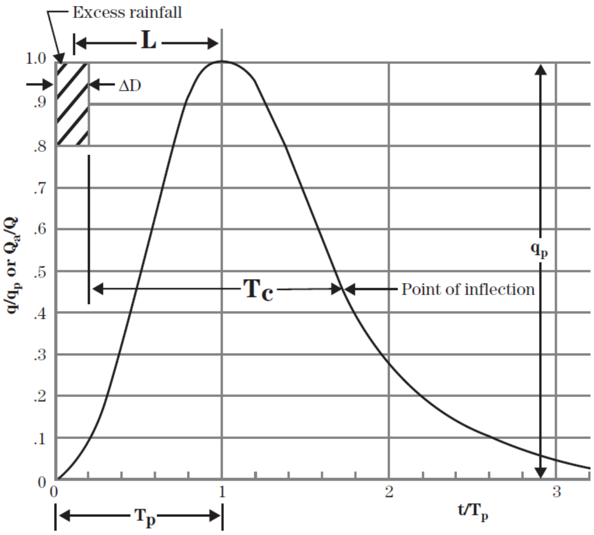

Figure 8: Relationship of time of concentration and lag time to the dimensionless unit hydrograph (NRCS 2010).

Flow Routing

A Muskingum-Cunge procedure was used to route flow from upper catchments to the stream outlets. This 1-dimensional method, embedded in HEC-HMS, allows for flow attenuation in the computations but does not provide a numerical solution of the full unsteady flow routing equations, as provided in such computational models as HEC-RAS. In each reach, flow routing was estimated using a single simplified cross section, channel slope, and Manning's *n* estimates. Manning's *n* was selected to maintain subcritical or approximately critical velocity, reflecting an assumption that existing or new channel bedform development prevents reach-average supercritical flow.

The model used in the BAER process (WILDCAT) does not allow flow routing; composite watersheds were instead developed to estimate flow at catchment outlets, potentially violating CN methodology requirements for larger catchments.

Sediment Bulking

A simple multiplication factor was applied to the post-fire flood predictions to account for sediment bulking in the debris flows. For burned catchments, this multiplication factor was assumed to be 1.25 if the severe + moderate (S+M) soil burn severity aerial extent was greater than 50%, and 1.1 for catchments with between 10 and 50 % S+M soil burn severity.

Streamstats

The regional USGS regression equations for peak flow prediction (Capesius and Stephens 2009), embedded in Streamstats, were used to assess the reasonableness of pre-fire peak flow predictions. For elevations below 7500 feet, where rainfall from convective storms are assumed to be dominant in runoff, peak flow is predicted by

$$
\begin{aligned}
Q_2 &= 10^{1.26} A^{0.52} P_{100}^{0.35} \\
Q_{10} &= 10^{0.85} A^{0.59} P_{100}^{2.15} \\
Q_{25} &= 10^{0.84} A^{0.61} P_{100}^{2.57} \\
Q_{50} &= 10^{0.85} A^{0.62} P_{100}^{2.79} \\
Q_{100} &= 10^{0.88} A^{0.63} P_{100}^{2.98}
\end{aligned}
$$

, where Q is the peak flow estimate (cfs), the subscript is the recurrence interval (years), A is the drainage area (mi^2) and P_{100} is the 6-hour, 100-year precipitation depth (inches). The error bars associated with these predictions are substantial – typically about 140 percent.

These predictions are based on actual streamgage data and, hence, provide a level of ground truthing, but this method accounts for only drainage area and precipitation regime. Other physical characteristics and processes that are relevant in runoff processes, such as infiltration capacity, vegetative type, ground cover condition, watershed shape, and flow attenuation, are not accounted for. However, due to its foundation in actual data, this method is valuable for assessing the general reasonableness of the model predictions of pre-fire conditions.

RESULTS and DISCUSSION

The purpose of this modeling was to develop estimates of flood hazard potential and potential threats to life and property along streams draining the High Park Fire. These results are reasonable predictions for the determination of sufficiency of the current infrastructure for passing increased flood flows, as well as allow design of new infrastructure. These results can also be used to compute values useful for stream stability assessment, such as stream power.

In many catchments, post fire conditions are predicted to cause a 50- or 100-year (pre-fire) flood to result from a 10-year rain event on burned landscapes, similar to actual measured fire runoff responses (Conedera et al. 2003). Peak flow predictions for individual streams are provided in the maps presented in Appendix A. Pre-fire and post-fire peak flows, an estimate of the expected sediment-bulking flow, and post/pre fire peak flow ratios are presented for the 2-, 10-, 25-, 50-, and 100-year rain events. Example hydrographs for pre- and post-fire conditions at the catchment outlets are also provided. Soil burn severity is also shown on the mapping, along with modeled junctions and stream reaches.

Accompanying the results presented in Appendix A is a poster that shows the expected increase in flood potential of almost all of the streams draining the High Park Fire. This focus of this poster is post/pre fire peak flow ratios, which is simply computed as the post-fire peak flow divided by the pre-fire peak flow, as computed at each individual or nested catchment outlet point. Also included in this poster are the soil burn severity imagery and a summary of the methodology used in the computations.

Example Hydrographs

Hydrographs are plots of flow versus time. For several key catchments draining the High Park Fire, hydrographs are provided (Figures 9 and 10) that show the expected response to a 10-year rain event over each entire catchment for pre- and post- fire conditions. Substantially higher peak flows and flood volumes have been modeled for post-fire conditions.

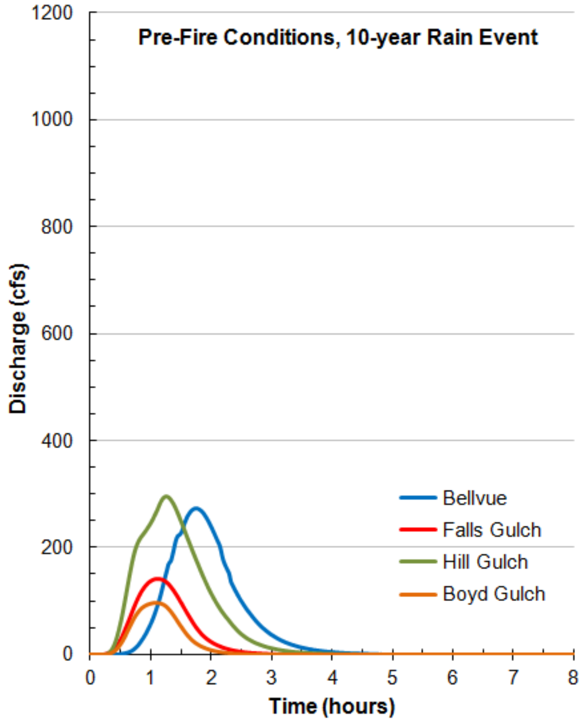

Figure 9: Selected pre-fire hydrographs, 10-year rain event.

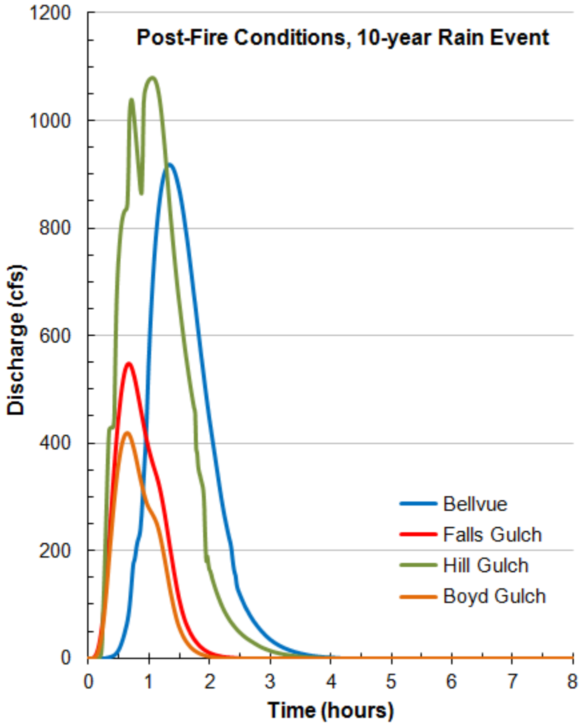

Figure 10: Selected post-fire hydrographs, 10-year rain event.

If it is assumed that the fire impacts on runoff in each of these catchments will be substantial for at least 5 years, the risk of a 10-year rain event over each individual point in these catchments over those 5 years of destabilization is 41 percent, with resulting (pre-fire) 50- and 100-year floods. However, as catchment size increases the small spatial extent of typical convective storms will reduce the severity of the flood effects from these storms.

Fire Severity

As computed using the CSU BARC image, for areas that were burned in the modeled catchments, 21 percent were burned at high severity, 52 percent at moderate severity, and 27 percent at low severity. This fire is considered a dirty burn, with numerous patches of unburned areas within the overall fire perimeter. Within the modeled extent (which included unburned areas both within and downstream of the burn perimeter), on average 13 and 33 percent of the catchments were burned at high and moderate soil burn severities, respectively.

Comparison with Regression Predictions

Table 2 illustrates USGS regression modeling results (from Streamstats) compared to CN modeling results at key locations for the 10- and 25-year events. As discussed above, these regression predictions are based on actual streamgage data but accounts for only drainage area and precipitation regime. Relevant hydrologic processes not addressed in the regression equations include soil infiltration capacity, vegetative type, ground cover condition, watershed shape, and stream flow attenuation.

Considering the large expected prediction error of the USGS regression equations (typically 140%), the results are reasonably comparable, with some catchments and return intervals being quite similar. The greatest differences in prediction are in Buckhorn and Redstone Creeks (CN predictions substantially less than regression results), and Young Gulch (CN predictions substantially greater than regression results). For the 50- and 100-year events, the CN modeling results tend to increase in comparison with the regression modeling results, becoming more in line with each other in the Buckhorn and Redstone catchments and becoming more divergent in Young Gulch.

Table 2: Comparison of CN modeling with USGS regressions published in Streamstats. Reg: regression result; MC: Mill Canyon; BC: Buckhorn Creek; HlG: Hewlett Gulch; LC: Lewstone Creek; CG: Cedar Gulch; SG: Stevens Gulch; PC: Pendergrass Creek; PG: Poverty Gulch; FG: Fall Gulch; HG: Hill Gulch; BG: Boyd Gulch; UN: Unnamed; RdC: Redstone Creek; RC: Rist Canyon; SG: Skin Gulch; YG: Young Gulch.

	Area	10-yr flow (cfs)		25-yr flow (cfs)	
Point	**(mi^2)**	**CN**	**Reg**	**CN**	**Reg**
MC-2	3.33	119	212	249	360
MC-5	6.61	272	335	588	574
BC-8	23.2	44	407	119	650
BC-13	42.9	244	599	474	974
BC-18	55.0	332	741	729	1230
HIG-3	10.9	207	248	446	387
HIG-5	21.8	210	348	466	554
LC-1	1.20	23	96	60	152
LC-4	6.97	168	277	354	460
CG	2.00	89	92	178	139
SG	1.73	19	81	59	121
PC-3	5.13	147	150	264	227
PG-3	4.31	121	136	242	206
FG	1.33	140	93	238	146
HG-3	5.53	296	226	564	368
BG	1.22	97	95	177	151
UN-3	0.28	21	40	42	61
RdC-2	5.05	131	231	284	382
RdC-5	13.2	180	445	479	764
RdC-6	16.2	168	512	478	885
RC-2	3.00	172	170	334	277
RC-4	8.16	282	316	549	531
SG-1	3.09	103	120	216	183
SG-2	1.19	45	73	96	111
SG-4	5.99	191	182	395	283
YG-3	7.22	448	218	820	345
YG-5	1.22	36	95	82	150
YG-6	12.4	537	317	1057	512
YG-7	15.2	550	361	1100	586

Time-to-Peak Estimates

For emergency response purposes, it is helpful to have an understanding of the expected flood response time within catchments. For this purpose, time-to-peak estimates (T_p) are provided (Table 3). As shown in Figure 8, the time-to-peak is from the start of the rainfall to the peak flow. Estimates are provided for key points within the catchments, for the 10- and 25-year events. It is important to remember that these values are based on the assumption that rain storms are over entire catchments; spatially variable convective storms may shorten the actual time to peak flow.

Table 3: Time to peak estimates at selected points on streams draining the High Park Fire. Refer to Appendix A mapping for point locations. Q_p: post fire peak discharge; T_p: post fire time to peak

Location		10-year		25-year		Location		10-year		25-year	
	Area (mi^2)	Q_p (cfs)	T_p (min)	Q_p (cfs)	T_p (min)		Area (mi^2)	Q_p (cfs)	T_p (min)	Q_p (cfs)	T_p (min)
MC-2	3.33	430	65	690	62	Falls Gulch	1.33	550	40	770	38
Long-Brown Gulch	2.64	380	68	600	66	HG-1	3.61	630	50	980	49
North Mill Canyon	1.13	93	74	160	70	Watha Gulch	1.12	580	32	810	30
MC-5	6.61	920	81	1500	76	HG-3	5.53	1100	64	1700	52
Empire Gulch	0.48	72	55	120	52	Boyd Gulch	1.22	420	39	610	37
Soldier Canyon	0.74	100	55	170	52	Unnamed 2	1.17	360	43	520	42
BC-1	1.34	54	71	110	62	Unnamed 3	0.28	130	21	200	20
Buckhorn Creek F	1.85	110	72	200	68	Unnamed 4	0.20	48	37	74	36
Whitepine A	1.02	31	71	56	66	Unnamed 5	0.09	17	34	27	33
Buckhorn Creek K	1.48	140	62	230	58	Unnamed 6	0.21	55	33	82	32
BC-8	23.2	170	64	310	112	RdC-1	1.35	260	43	410	42
BC-10	2.08	79	78	160	74	Blackhurst Gulch	2.27	150	90	270	88
BC-11	31.1	360	47	690	91	RdC-2	5.05	490	63	800	60
Buckhorn Creek O	1.65	280	55	420	54	Raspberry Gulch	2.79	140	86	260	82
BC-13	42.9	620	96	1100	85	RdC-3	8.93	660	84	1100	79
BC-14	1.64	140	62	240	57	RdC-4	2.30	180	73	320	68
BC-15	4.97	390	85	680	79	RdC-5	13.2	880	102	1600	92
BC-16	50.2	870	137	1700	117	RdC-6	16.2	880	134	1600	117
BC-18	55.0	810	213	1600	187	RC-1	1.44	330	46	490	44
Hewlett Gulch C	1.13	170	52	270	50	RC-2	3.00	630	58	970	54
HIG-3	10.9	250	82	500	131	RC-3	5.14	860	77	1400	76
HIG-5	17.4	300	147	610	121	Rist D	1.77	520	51	750	50
HIG-6	21.8	310	197	650	169	RC-4	8.16	1000	74	1700	91
LC-1	1.20	92	71	170	65	SG-1	3.09	570	51	880	50
Lewstone Creek B	0.35	32	46	59	44	SG-2	1.19	190	47	310	45
Lewstone Creek D	1.79	550	43	800	42	SG-3	5.81	950	65	1500	59
LC-3	5.15	740	48	1100	47	SG-4	5.99	940	72	1500	64
LC-4	6.97	940	93	1400	87	Unnamed 14	0.28	41	36	69	35
Cedar Gulch	2.00	390	56	600	54	YG-1	1.94	230	57	390	54
Stevens Gulch	1.73	160	75	270	72	Young Gulch-C	2.14	510	50	750	49
Unnamed 13	0.11	10	35	20	34	Young Gulch-D	0.54	180	34	250	31
PC-1	3.52	440	64	730	60	YG-3	7.22	1100	64	1800	61
PC-3	5.13	610	84	1000	80	Young Gulch-F	0.67	120	49	180	47
PG-1	0.97	58	71	110	66	YG-5	1.22	160	52	260	48
PG-3	4.31	650	70	980	67	YG-6	12.4	1600	113	2700	80
						YG-7	15.2	1700	112	2900	102

Limitations in Modeling Accuracy

The conceptual foundation of the CN technique can be disconnected with the physical streamflow generating processes, especially during more-frequent small to moderate rain events in forested watersheds. An assumption inherent in the CN technique is that catchment runoff is driven by infiltration-excess overland flow, where surface runoff is generated when rainfall intensity is greater than soil infiltration capacity. This is generally valid in arid and semi-arid regions, in post-fire conditions, and during higher rainfall depths and intensities. In contrast, saturation excess overland flow, where rainfall depths exceed the soil capacity to retain water and becomes saturated and producing runoff from relatively small and variable portions of a catchment, can be typically dominant in unburned forested watersheds for frequent (shallow) rain events.

Additionally, scale effects are relevant in post-fire runoff prediction, with greater actual runoff enhancement in smaller catchments and tendencies towards overestimation in larger catchments. This may likely be due in part to repercussions associated with the limited spatial extent of convective storms.

Additionally, due to apparently biased hydrologic soil group classifications towards having excessive infiltration capacity, catchments draining the Arapaho-Roosevelt soil survey area (South Fork Cache la Poudre, western Skin Gulch, upper Pendergrass and Poverty, upper Buckhorn Creek) are likely underpredicting runoff, especially for more frequent (shallower) rain events. In the most problematic areas zero runoff is predicted for pre-fire conditions in some catchments during the 10- and 25-year rain events. This problem may be due to shallow, permeable soils over bedrock dominating the soil survey classification methodology. The ramification of this HSG classification problem will decrease for less frequent (deeper) rain events.

Hence, these modeling results are likely to have greater accuracy for smaller catchments and less frequent (deeper) rain events, but overpredict as catchment size increases and underpredict for more-frequent (shallower) rain events.

CONCLUSIONS

Using the NRCS Curve Number method, peak flow predictions were made for streams draining the High Park Fire, for both pre-fire and post-fire conditions. Watershed maps for each modeled catchment were developed, illustrating computation points, soil burn severity, and 10-year hydrographs at the stream outlet. Tables with expected pre- and post-fire peak flows, sediment bulking flows, and post/pre fire peak flow ratios were also provided on these watershed maps. An overall poster illustrating increased flood potential of streams draining the fire was also developed. The specific modeling accuracy is unknown, though predictions are likely to be more accurate in smaller catchments and for less-frequent (deeper) rain events.

ACKNOWLEDGEMENTS

Appreciation is expressed to Claudia Hoeft for report review, and post-fire CN assignment compilation and report review by John Andrews. Appreciation is also expressed to Brandon Stone and Colorado State University for the revised (7/20) BARC soil burn severity interpretation, John Norman for GIS analysis assistance and soils expertise, and Kari Sever and Sam Streeter for field data collection.

REFERENCES

BAER 2012 *High Park Fire Burned Area Emergency Response Report* USDA USFS and NRCS, Larimer County, Colorado Department of Transportation, July 17th.

Benavides-Solorio, J., MacDonald, L.H. 2001 *Post-Fire Runoff and Erosion from Simulated Rainfall on Small Plots, Colorado Front Range* Hydrological Processes 15, 2931-2952.

Capesius, J.P., Stephens, V.C. 2009 *Regional Regression Equations for Estimation of Natural Streamflow Statistics in Colorado* U.S. Department of Interior, U.S. Geological Survey, Scientific Investigations Report 2009-5136.

Conedera, M., Peter, L., Marxer, P., Forster, F., Rickenmann, D., Re, L. 2003 *Consequences of Forest Fires on the Hydrogeological Response of Mountain Catchments: A Case Study of the Riale Buffaga, Ticino, Switzerland* Earth Surface Processes and Landforms 28, 117-129.

Hudak, A.T., Robichaud, P.R., Evans, J.S., Clark, J., Lannom, K., Morgan, P., Stone, C. 2004 *Field Validation of Burned Area Reflectance Classification (BARC) Products for Post Fire Assessment* Remote Sensing for Field Users: Proceedings of the Tenth Forest

Service Remote Sensing Applications Conference, Salt Lake City, Utah, April 5-9 2004.

Huffman, E.L., MacDonald, L.H., Stednick, J.D. 2001 *Strength and Persistence of Fire-Induced Soil Hydrophobicity Under Ponderosa and Lodgepole Pine, Colorado Front Range* Hydrological Processes 15, 2877-2892.

Maidment, D.R. 1992 *Handbook of Hydrology* McGraw-Hill, Inc.

Miller, J.F., Frederick, R.H., Tracey, R.J. 1973 *Precipitation-Frequency Atlas of the Western United States*. U.S. Department of Commerce, National Oceanic and Atmospheric Administration, National Weather Service, NOAA Atlas 2, Vol 3, Silver Spring, Maryland.

NRCS 2004a *Hydrologic Soil Cover Complexes* USDA Natural Resources Conservation Service, National Engineering Manual, Chapter 9, 210-VI-NEH, July.

NRCS 2004b *Estimation of Direct Runoff from Storm Rainfall* USDA Natural Resources Conservation Service, National Engineering Manual, Chapter 10, 210-VI-NEH.

NRCS 2010 *Time of Concentration* USDA Natural Resources Conservation Service, National Engineering Manual, Chapter 15, 210-VI-NEH.

Rallison, R.E. 1980 *Origin and Evolution of the SCS Runoff Equation* Proceedings of the Symposium on Watershed Management; American Society of Civil Engineers, Boise, ID.

Stoof, C.R., Vervoort, R.W., Iwema, J., van den Elsen, J., Ferreira, A.J.D., Ritsema, C.J. 2011 *Hydrological Response of a Small Catchment Burned by an Experimental Fire* Hydrology and Earth System Sciences Discussions 8, 4053-4098.

Woodward, D 2005 Personal Communications (email), Retired National Hydraulic Engineer, USDA Natural Resources Conservation Service, Washington D.C.